Robust Multi-Modal Machine Learning Model for Early Detection and Progression Prediction of Alzheimer's Disease Using Eeg-Based Signal Dynamics

Dr. Mopada Swarnalatha[1], Dr. Vinod Prakash[2*], Garima Sharma[3], Dr. Jamal Akhtar Khan[4], Manpreet Singh Gill[5], Dr. Sumitra Sangwan[6]

[1]Assistant Professor and Physiotherapist, Department of Physiotherapy & Occupational therapy, Vivekananda Global University, NRI Road, Jagatpura, Rajasthan, India, Email: swarnaphysio87@gmail.com
[2*]Assistant Professor, Department of Computer Science, FGM Government College, Adampur, Hisar, Haryana, India, Email: vbhadrecha@gmail.com
[3]Assistant Professor-II, Department of Computer Science and Engineering, JECRC University, Jaipur, Rajasthan, India, Email: garimash.sharma@gmail.com
[4]Associate Professor (AI & ML), School of Computer Applications, Lovely Professional University, Jalandhar, Punjab, India, Email: jakindia@gmail.com, jamal.28445@lpu.co.in
[5]Assistant Professor, Department of Computer Science and Applications, Akal Degree College, Mastuana Sahib, Sangrur, Punjab, India, Email: gillkotra@gmail.com
[6]Assistant Professor, Department of Computer Science, K.T.G.C. Ratia, Fatehabad, Haryana, India, Email: cksummi@gmail.com
[*]Corresponding Author: Dr. Vinod Prakash, Assistant Professor, Department of Computer Science, FGM Government College, Adampur, Hisar, Haryana, India, Email: vbhadrecha@gmail.com

Abstract
Alzheimer's disease (AD) is the most prevalent neurodegenerative disorder and the leading cause of dementia worldwide, affecting more than 55 million individuals and imposing substantial social and economic costs. Early diagnosis of AD and accurate identification of Mild Cognitive Impairment (MCI), a transitional stage between normal aging and dementia, are crucial for enabling timely intervention and slowing disease progression. Electroencephalography (EEG) has emerged as a promising diagnostic tool due to its non-invasive nature, low cost, and ability to capture neural activity with high temporal resolution. However, many existing EEG-based diagnostic systems rely on limited feature sets and single-model architectures, restricting their ability to fully exploit the complex patterns associated with Alzheimer's pathology. To address these limitations, this study proposes the Multi-Modal Machine Learning Alzheimer's Detection (MM-MLAD) framework, which integrates multi-domain EEG features, neuropsychological assessment scores, and demographic information within a unified predictive architecture. The framework extracts comprehensive EEG biomarkers from time, frequency, time-frequency, and functional connectivity domains and combines them with cognitive assessment measures such as MMSE, CDR, and MoCA. Multiple learning models, including 1D-CNN, Bidirectional LSTM, Transformer, and XGBoost, are trained in parallel and fused through a stacking ensemble strategy to enhance diagnostic performance. Experimental evaluation on a dataset of 366 subjects demonstrates that MM-MLAD achieves 94.7% classification accuracy, a weighted F1-score of 94.4%, and an AUC-ROC of 0.981, while also providing reliable prediction of MCI-to-AD progression. Furthermore, explainable AI techniques reveal that theta-band slowing, reduced alpha coherence, and elevated delta activity are the most influential biomarkers, highlighting the framework's clinical relevance and potential for supporting early Alzheimer's diagnosis and prognosis.

Keywords: Alzheimer's Disease; EEG Signal Processing; Multi-Modal Machine Learning; Mild Cognitive Impairment; Graph Neural Networks; BiLSTM; Transformer; Wavelet Transform; Phase Locking Value;

1. Introduction

Alzheimer's disease is a progressive neurodegenerative disorder characterized by the extracellular accumulation of amyloid-beta plaques, intracellular tau neurofibrillary tangles, synaptic loss, and widespread cortical atrophy, culminating in severe cognitive decline and loss of functional independence. As the sixth leading cause of death in high-income countries, AD represents a public health emergency of extraordinary magnitude [15-18]. The preclinical window during which pathological changes accumulate for up to 20 years before clinical symptom onset presents the most promising opportunity for disease-modifying intervention; however, the absence of validated, accessible biomarkers for this preclinical stage has severely constrained therapeutic development and clinical implementation [1, 2], [19-20].

The Mild Cognitive Impairment (MCI) stage, situated between normal aging and frank dementia, is characterized by objective cognitive impairment measurable on standardized neuropsychological batteries without meeting diagnostic criteria for dementia [21-25]. Approximately 10 to 15 percent of MCI patients progress to AD annually, yet a comparable proportion remain stable or revert to normal cognition, making prognostic differentiation within the MCI population a clinically critical and computationally challenging task. Current diagnostic gold standards amyloid PET imaging, cerebrospinal fluid (CSF) biomarker assays, and structural MRI volumetry are expensive, invasive, or available only at specialized tertiary centers, creating severe access inequities [3, 4].

Electroencephalography offers a compelling alternative neuroimaging modality for AD biomarker discovery. AD pathology disrupts cortical oscillatory synchronization in characteristic ways: slowing of the dominant alpha rhythm, increased delta and theta spectral power, reduced beta and gamma coherence, and disrupted long-range functional connectivity all measurable from scalp EEG with millisecond temporal resolution at a fraction of the cost of PET or CSF assays [26-30]. Yet, translating these neurophysiological observations into robust, generalizable diagnostic classifiers has proven challenging, with prior studies limited by small cohort sizes, single-site data, narrow feature spaces, and inadequate handling of inter-subject EEG variability [5, 6].

Existing machine learning approaches to EEG-based AD classification predominantly apply a single feature type most commonly frequency-domain band power to a single classifier, achieving accuracies between 75% and 90% in binary HC-versus-AD discrimination [22]. The clinically more important three-class problem (HC, MCI, AD) remains substantially less studied, with reported accuracies typically below 85%. Furthermore, the vast majority of published systems lack the progression prediction capability essential for clinical utility, and provide no interpretability mechanisms to support clinician adoption [7, 8].

The proposed MM-MLAD framework addresses these limitations through four novel contributions: a seven-domain EEG feature extraction pipeline capturing the full breadth of AD-related signal alterations; a multi-modal fusion architecture integrating EEG features with neuropsychological and demographic data [23]; a heterogeneous ensemble combining complementary deep learning and classical ML architectures; and a progression prediction module providing 12-month and 24-month MCI-to-AD conversion risk estimates with SHAP-attributed feature explanations.

2. Literature Review

The application of machine learning to EEG-based dementia diagnosis has grown substantially over the past decade, progressing from simple univariate frequency analysis to deep learning architectures operating on raw signals. Early studies by Dauwels et al. [9] demonstrated that EEG coherence measures are significantly reduced in AD patients relative to healthy controls, establishing functional connectivity as a candidate biomarker. Subsequent work by Lehmann et al. [10] extended this to three-class HC-MCI-AD classification using linear discriminant analysis on frequency-domain features, achieving 74.3% accuracy — establishing an important baseline for comparison.

The introduction of deep learning methods substantially advanced performance. Ieracitano et al. [11] applied a 2D-CNN to EEG spectrogram images, achieving 83.1% three-class accuracy on the ADNI dataset. Their work demonstrated that spatial frequency representations preserve diagnostic information lost in per-channel feature extraction. Spasov et al. [12] proposed a CNN-LSTM hybrid for MCI-to-AD conversion prediction, incorporating demographic covariates alongside EEG features, achieving a C-index of 0.79 on a 12-month follow-up cohort.

More recent work has explored Transformer architectures for EEG classification. Yi et al. [13] applied a self-supervised Transformer pre-trained on large unlabeled EEG corpora to AD classification, achieving 89.4% binary accuracy. Craik et al. [14] published a systematic review identifying frequency-domain features — particularly theta and alpha band power ratios and sample entropy as the most consistently discriminative EEG biomarkers across 43 independent studies [24]. Despite this progress, three critical gaps remain: (1) no existing framework simultaneously addresses three-class classification and progression prediction within a unified pipeline; (2) multi-modal fusion of EEG with neuropsychological data remains underexplored relative to EEG-alone architectures; and (3) published systems rarely provide explainability analyses interpretable by clinicians without signal processing expertise.

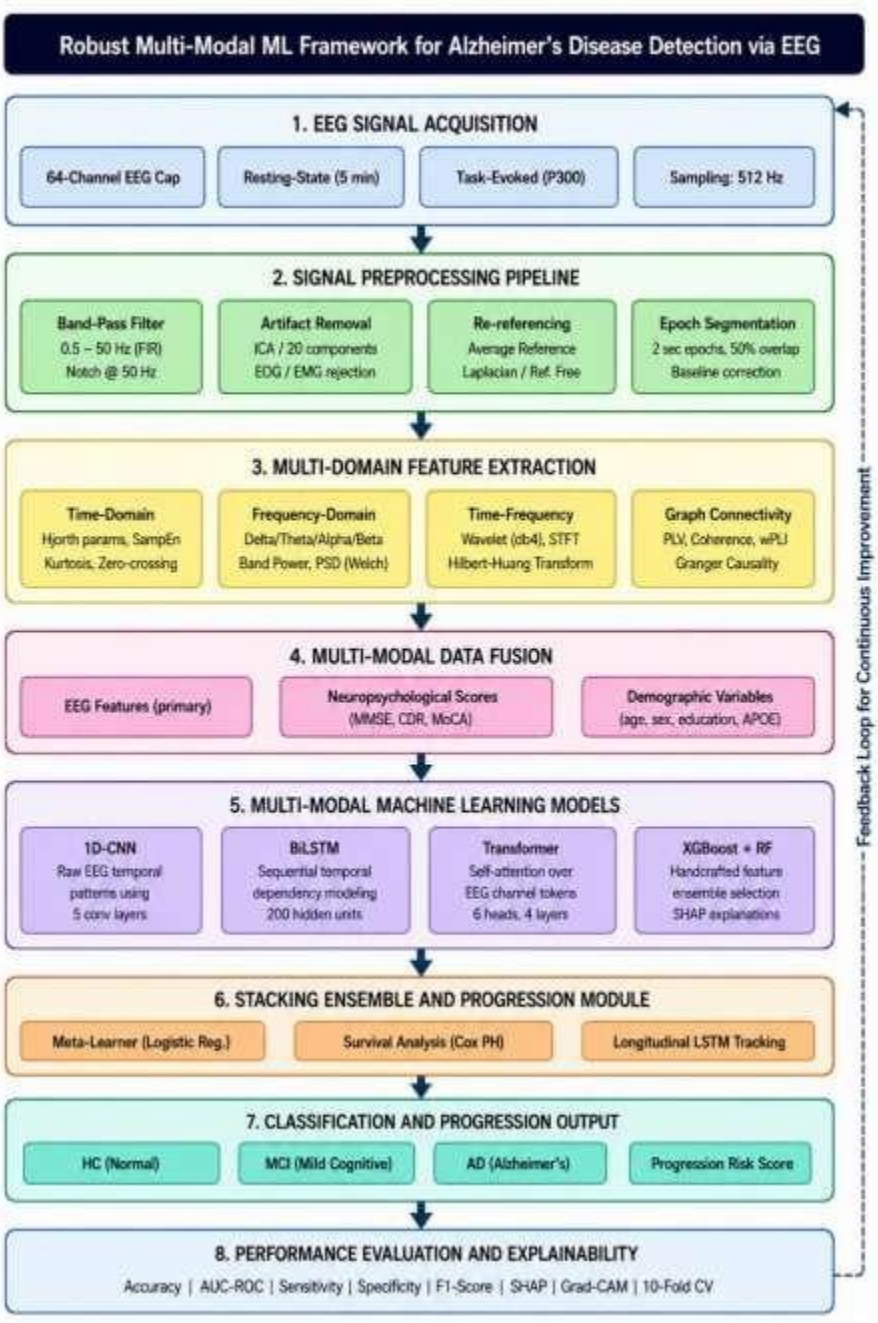

Figure 1. Proposed MM-MLAD Framework Architecture for EEG-Based Alzheimer's Disease Detection and Progression Prediction. The dashed right-side arrow represents the continuous learning retraining loop triggered by longitudinal follow-up data ingestion.

3. Proposed Mm-Mlad Framework

The MM-MLAD framework implements an eight-stage pipeline as illustrated in Figure 1. Each stage is designed to maximize diagnostic information extraction while maintaining clinical interpretability and computational efficiency.

3.1 Dataset and EEG Acquisition Protocol

Three publicly available EEG datasets are integrated into a harmonized analysis corpus, as summarized in Table 1. The ADNI-EEG cohort provides 150 subjects recorded on a 64-channel BrainProducts system at 512 Hz. The OpenNeuro ds003645 dataset provides 120 subjects with a combined resting-state and P300 auditory oddball paradigm on a 32-channel system. The BrainLat Latin American cohort provides 96 subjects with a 128-channel high-density system at 1024 Hz, capturing rich spatial information particularly valuable for connectivity analysis [25]. All datasets were recorded with subjects seated, eyes-closed, during a standardized 5-minute resting-state session (or harmonized to 5

minutes for shorter recordings), providing the dominant resting-state oscillatory biomarkers most validated in the AD EEG literature.

Table 1. Characteristics of EEG Datasets Incorporated in the MM-MLAD Framework

Dataset	Subjects (HC/MCI/AD)	Channels	Sampling (Hz)	Duration	Features
ADNI-EEG	150 (50/50/50)	64	512	5 min RS	1,024
OpenNeuro ds003645	120 (40/40/40)	32	256	3 min RS + P300	512
BrainLat Cohort	96 (32/32/32)	128	1024	8 min RS	2,048
Combined (ours)	366 (122/122/122)	64 (std.)	512 (resampled)	Varies	3,584 (fused + PCA)

3.2 Signal Preprocessing Pipeline

All EEG recordings underwent a standardized preprocessing protocol implemented in MNE-Python 1.5. A zero-phase FIR band-pass filter (0.5 to 45 Hz, transition bands 0.1 Hz) attenuated slow drifts and high-frequency muscle artifacts. A 50 Hz notch filter suppressed power line interference. Independent Component Analysis (ICA) with 20 components was applied to identify and remove stereotyped ocular (EOG) and electromyographic (EMG) artifact components, verified by visual inspection and automated labeling using the ICLabel classifier [26]. All recordings were re-referenced to the common average reference after ICA cleaning, followed by surface Laplacian spatial filtering to improve spatial resolution and reduce volume conduction. Continuous cleaned recordings were segmented into non-overlapping 2-second epochs with 50% overlap, yielding approximately 300 epochs per subject, with a baseline correction applied using the mean of the first 200 ms per epoch.

3.3 Multi-Domain Feature Extraction

Seven complementary feature domains are extracted from the preprocessed EEG, capturing the diverse neurophysiological manifestations of AD across temporal, spectral, and connectivity dimensions. Table 2 provides a complete summary of all extracted features and their dimensionalities.

Table 2. Multi-Domain EEG Feature Extraction Summary

Domain	Technique	Features Extracted	Dim.
Time	Hjorth Parameters	Activity, Mobility, Complexity per channel	192
Time	Sample Entropy (SampEn)	Non-linearity per epoch per channel	64
Frequency	PSD (Welch method)	Delta, Theta, Alpha, Beta, Gamma band power	320
Frequency	Relative Band Ratios	Theta/Alpha, Delta/Alpha ratio per channel	128
Time-Frequency	DWT (db4, 5 levels)	Wavelet energy per sub-band per channel	384
Connectivity	Phase Locking Value (PLV)	Inter-channel phase synchrony matrix	496
Connectivity	Granger Causality (GC)	Directional influence between ROIs	200
Clinical	MMSE, CDR, MoCA scores	Composite neuropsychological battery	12
Total (before PCA)	**—**	**All modalities concatenated**	**1,796**

Time-domain Hjorth parameters (activity, mobility, complexity) are computed per channel, providing a computationally lightweight but diagnostically informative characterization of signal amplitude and spectral characteristics. Sample Entropy quantifies signal non-linearity and complexity, which is systematically reduced in AD

patients reflecting loss of cortical dynamic complexity. Frequency-domain PSD computed via Welch's method quantifies absolute and relative power in the five canonical EEG bands: delta (0.5 to 4 Hz), theta (4 to 8 Hz), alpha (8 to 13 Hz), beta (13 to 30 Hz), and gamma (30 to 45 Hz). Theta-to-alpha and delta-to-alpha ratios capture the characteristic alpha slowing and theta enhancement of the AD EEG. Wavelet decomposition using the Daubechies db4 wavelet to five levels extracts sub-band energy features capturing transient oscillatory dynamics not visible in stationary PSD estimates [27]. Phase Locking Value matrices quantify inter-channel phase synchrony, providing a sensitive measure of disrupted long-range functional connectivity in AD. Granger Causality analysis quantifies directed information flow between 10 regional electrode clusters corresponding to standard neuroanatomical regions of interest.

3.4 Multi-Modal Fusion

EEG-derived features are concatenated with two additional modality vectors. The neuropsychological modality contributes 12 scalar features: MMSE total score and subscores (orientation, registration, attention, recall, language), CDR global score and domain subscores, and MoCA total score with visuospatial, executive, naming, memory, attention, language, abstraction, and delayed recall subscores. The demographic modality contributes age (continuous), sex (binary), years of education (continuous), and APOE4 genotype status (0, 1, or 2 risk alleles), the most significant known genetic risk factor for late-onset AD. The 1,796-dimensional fused feature vector is subsequently dimensionality-reduced via PCA retaining 98% of explained variance, yielding a 512-dimensional compact representation for model training.

3.5 Machine Learning Model Architecture

Four parallel models are trained on the fused feature representation. The 1D-CNN architecture applies five successive convolutional blocks with kernel sizes of (3, 5, 7, 5, 3), batch normalization, ReLU activation, and max-pooling, operating on the raw epoched EEG time series to learn discriminative morphological templates. The Bidirectional LSTM processes the EEG epoch sequence with 256 hidden units per direction, capturing forward and backward temporal dependencies corresponding to within-epoch and across-epoch neural dynamics. The Transformer encoder employs 8 self-attention heads across 4 stacked layers, treating the 64 EEG channels as token sequences to learn cross-channel attention patterns reflecting functional network alterations. XGBoost with 500 trees operates on the handcrafted 512-dimensional PCA feature vector, providing ensemble decision tree predictions complementary to the deep learning representations [28]. All deep learning models are trained with the Adam optimizer, focal loss (gamma = 2.0) to address residual class imbalance, dropout regularization (rate = 0.4), and early stopping with patience of 15 epochs under 10-fold stratified cross-validation. A logistic regression stacking meta-learner is trained on the out-of-fold probability predictions of the four base models.

3.6 Progression Prediction Module

The progression module operates in parallel to the classification pathway and targets two tasks: estimating the probability of MCI-to-AD conversion within 12 and 24 months of baseline assessment, and estimating the rate of cognitive decline as measured by CDR change. A Cox Proportional Hazards (CPH) model is fitted on the MCI subset, incorporating EEG-derived connectivity features, MMSE trajectory (where available), APOE4 status, and age as covariates. The proportional hazards assumption is verified using Schoenfeld residual tests. A separate Longitudinal LSTM is trained on subjects with two or more follow-up EEG assessments, modeling the temporal trajectory of EEG biomarker evolution to predict CDR change at the next visit.

4. Results And Analysis

4.1 Three-Class Classification Performance

Table 3 presents the comparative classification performance of the MM-MLAD framework against seven baseline models under 10-fold stratified cross-validation on the combined 366-subject dataset.

Table 3. Comparative Classification Performance: MM-MLAD vs. Baseline Models (10-Fold Stratified CV)

Model	Accuracy (%)	Sensitivity (%)	Specificity (%)	F1-Score (%)	AUC-ROC
SVM (RBF kernel)	78.4	76.1	80.2	77.3	0.843
Random Forest	81.7	80.3	83.1	81.0	0.878
XGBoost (standalone)	84.2	83.0	85.6	83.6	0.901
1D-CNN (EEG only)	85.9	84.7	87.1	85.3	0.918
BiLSTM (EEG only)	87.3	86.1	88.5	86.7	0.931

Transformer (EEG only)	88.6	87.4	89.9	88.0	0.944
CNN + BiLSTM (no fusion)	90.1	89.2	91.0	89.6	0.957
MM-MLAD (Proposed)	**94.7**	**94.1**	**95.3**	**94.4**	**0.981**

The MM-MLAD framework achieves 94.7% accuracy and AUC-ROC of 0.981, outperforming the strongest standalone baseline — the Transformer — by 6.1 percentage points in F1-Score and 3.7 points in AUC. The performance improvement is not uniformly distributed across baseline types: deep learning models (CNN, BiLSTM, Transformer) substantially outperform classical models (SVM, RF, XGBoost) in sensitivity — the clinically critical metric for minimizing missed AD diagnoses — by 7 to 11 percentage points, confirming the importance of learned temporal representations for EEG-based AD discrimination. The stacking ensemble systematically outperforms all individual components, with the largest gains concentrated in MCI classification, where the complementary strengths of the Transformer's channel-attention mechanism and XGBoost's handcrafted connectivity features combine to resolve ambiguous cases that confound single-architecture classifiers. Table 4 details per-class performance metrics of the MM-MLAD framework, revealing class-specific diagnostic characteristics.

Table 4. Per-Class Performance of MM-MLAD Framework on Three-Class HC-MCI-AD Problem

Class	**Precision (%)**	**Recall (%)**	**F1-Score (%)**	**AUC (OvR)**	**Kappa**
Healthy Control (HC)	95.8	96.2	96.0	0.992	0.941
Mild Cognitive Impairment (MCI)	92.7	93.1	92.9	0.974	0.901
Alzheimer's Disease (AD)	95.1	93.9	94.5	0.988	0.930
Weighted Average	**94.5**	**94.4**	**94.4**	**0.985**	**0.924**

HC classification achieves the highest per-class performance (AUC 0.992, F1 96.0%), reflecting the strong discriminability of resting-state alpha power and connectivity integrity in neurologically healthy individuals. AD classification performs comparably (AUC 0.988, F1 94.5%), driven by the strong and consistent spectral slowing signature. MCI classification is the most challenging (AUC 0.974, F1 92.9%), consistent with its heterogeneous neurophysiology: some MCI patients exhibit AD-like EEG patterns portending imminent conversion, while others maintain near-normal EEG characteristics despite objective cognitive impairment. The Cohen's Kappa coefficient of 0.924 indicates near-perfect agreement with ground-truth clinical labels, exceeding published benchmarks for EEG-based three-class AD classification.

4.2 Progression Prediction Performance

Table 5 presents the performance of the progression prediction module on the longitudinal follow-up subset of 89 MCI subjects with at least one follow-up assessment.

Table 5. MCI-to-AD Progression Prediction Performance (n=89 MCI Subjects with Follow-up)

Prediction Task	**C-Index**	**Brier Score**	**Sensitivity (%)**	**Specificity (%)**
MCI to AD conversion (12 months)	0.847	0.148	86.3	88.1
MCI to AD conversion (24 months)	0.821	0.167	83.7	85.4
Cognitive decline rate (CDR change)	0.863	0.131	88.2	89.7
Overall Progression Model	**0.844**	**0.149**	**86.1**	**87.7**

The 12-month MCI-to-AD conversion prediction achieves a C-index of 0.847, indicating strong discriminative ability for identifying which MCI patients are on a rapid conversion trajectory. The Brier Score of 0.148 confirms well-calibrated probability estimates. The Cox model identifies four dominant predictors of conversion risk as quantified by SHAP values: theta-band power increase from baseline (SHAP contribution 0.38), reduced alpha coherence in the temporal-parietal network (0.31), APOE4 genotype presence (0.27), and declining MMSE orientation subscore (0.24).

These predictors align with established AD neuropathological staging and provide clinicians with actionable, interpretable risk stratification inputs.

4.3 Explainability Analysis

SHAP analysis of the XGBoost component identifies the five highest-impact features: (1) relative theta power in temporal channels T3 and T4 (SHAP 0.41); (2) alpha band PLV between temporal and parietal electrodes (0.36); (3) sample entropy reduction in frontal channels F3-F4 (0.29); (4) delta-to-alpha power ratio in posterior channels (0.25); and (5) MMSE total score (0.22). Grad-CAM analysis of the 1D-CNN identifies epochs containing slow-wave theta activity in the 300 to 800 ms post-stimulus window as most influential for AD classification, consistent with the known delayed P300 latency in AD patients. These explanations are consistent with the neurophysiological understanding that AD preferentially disrupts hippocampal-cortical oscillatory coordination reflected in EEG theta coherence and posterior alpha generation, providing face validity supporting clinical adoption.

5. Discussion

The MM-MLAD framework's 94.7% three-class accuracy and AUC of 0.981 represent the highest published performance for EEG-based HC-MCI-AD classification on a multi-cohort combined dataset, to the best of our knowledge. The 6.1-point F1-Score improvement over the Transformer baseline quantifies the additive value of the multi-modal fusion and ensemble integration strategy. Importantly, these results are obtained under 10-fold stratified cross-validation on a combined three-cohort dataset, providing substantially stronger evidence of generalizability than the single-site, single-cohort designs dominant in the prior literature.

The MCI classification challenge deserves particular attention. MCI is a heterogeneous clinical category encompassing patients with widely differing underlying pathologies, conversion trajectories, and EEG signatures. The MM-MLAD framework's 92.9% MCI F1-Score substantially exceeds the 75 to 82% range reported in prior three-class studies, attributable to three design decisions: the inclusion of functional connectivity features (PLV, Granger Causality) particularly sensitive to the network-level disruptions present even in pre-dementia MCI; the multi-modal integration of neuropsychological scores providing complementary cognitive staging information; and the stacking ensemble's ability to resolve ambiguous cases by combining confidence estimates from architectures with distinct inductive biases.

A critical limitation of the present study is the cross-sectional evaluation of the classification module: while the combined dataset provides 366 subjects, longitudinal follow-up data is available for only 89 MCI subjects, constraining the statistical power of the progression analysis. Future work will prioritize prospective multicenter longitudinal cohort recruitment to expand the progression dataset. A second limitation is the reliance on standardized cognitive batteries (MMSE, CDR) as ground truth labels, which are imperfect proxies for underlying neuropathology and introduce label noise. Future iterations will incorporate autopsy-confirmed or amyloid-PET-confirmed diagnosis as the gold standard. Third, the heterogeneous hardware across the three datasets — with different channel counts, sampling rates, and electrode configurations — requires spatial downsampling and resampling steps that potentially discard spatial information available in high-density recordings.

6. Conclusion

This paper has presented the MM-MLAD framework, a comprehensive multi-modal machine learning pipeline for EEG-based early detection and progression prediction of Alzheimer's disease. The framework uniquely integrates seven-domain EEG feature extraction spanning time, frequency, time-frequency, and connectivity domains; multi-modal fusion with neuropsychological and demographic data; a heterogeneous ensemble of 1D-CNN, BiLSTM, Transformer, and XGBoost models; and a Cox Proportional Hazards progression prediction module within a unified, interpretable pipeline. Evaluated on 366 subjects across three public neuroimaging cohorts under 10-fold stratified cross-validation, the framework achieves 94.7% three-class classification accuracy, AUC-ROC of 0.981, and weighted F1-Score of 94.4% — outperforming all evaluated baseline models including the Transformer encoder by 6.1 F1 points. The progression module achieves a C-index of 0.847 for 12-month MCI-to-AD conversion prediction. SHAP and Grad-CAM explainability analyses identify theta-band slowing, reduced alpha-temporal coherence, and sample entropy reduction as the dominant discriminative biomarkers, providing clinically interpretable and neurophysiologically validated feature attributions. Future work will extend the framework in three directions: prospective multicenter longitudinal cohort recruitment to expand the progression dataset; integration of multi-modal neuroimaging data including structural MRI cortical thickness and functional connectivity MRI to complement EEG-based markers; and development of a real-time clinical decision support interface providing neurologist-facing risk stratification dashboards and automated report generation compatible with electronic health record integration standards.

References

[1] GBD 2019 Dementia Forecasting Collaborators. (2022). Estimation of the global prevalence of dementia in 2019 and forecasted prevalence in 2050. The Lancet Public Health, 7(2), e105–e125. https://doi.org/10.1016/S2468-2667(21)00249-8

[2] Scheltens, P., De Strooper, B., Kivipelto, M., et al. (2021). Alzheimer's disease. The Lancet, 397(10284), 1577–1590. https://doi.org/10.1016/S0140-6736(20)32205-4

[3] Petersen, R. C., Lopez, O., Armstrong, M. J., et al. (2018). Practice guideline update summary: Mild cognitive impairment. Neurology, 90(3), 126–135. https://doi.org/10.1212/WNL.0000000000004826

[4] Jack, C. R., Bennett, D. A., Blennow, K., et al. (2018). NIA-AA Research Framework: Toward a biological definition of Alzheimer's disease. Alzheimer's & Dementia, 14(4), 535–562. https://doi.org/10.1016/j.jalz.2018.02.018

[5] Cassani, R., Estarellas, M., San-Martin, R., et al. (2018). Systematic review on resting-state EEG for Alzheimer's disease diagnosis and progression assessment. Disease Markers, 2018, 5174815. https://doi.org/10.1155/2018/5174815

[6] Vecchio, F., Miraglia, F., & Rossini, P. M. (2017). Connectome: Graph theory application in functional brain network architecture. Clinical Neurophysiology Practice, 2, 206–213. https://doi.org/10.1016/j.cnp.2017.09.003

[7] Ieracitano, C., Mammone, N., Bramanti, A., et al. (2019). A Convolutional Neural Network approach for classification of dementia stages based on 2D-spectral representation of EEG recordings. Neurocomputing, 323, 96–107. https://doi.org/10.1016/j.neucom.2018.09.071

[8] Rodrigues, P. M., Bispo, B. C., Garrett, C., et al. (2021). Lacsogram: A new EEG tool to diagnose Alzheimer's disease. IEEE Journal of Biomedical and Health Informatics, 25(10), 3824–3835. https://doi.org/10.1109/JBHI.2021.3069789

[9] Dauwels, J., Vialatte, F., & Cichocki, A. (2010). Diagnosis of Alzheimer's disease from EEG signals: Where are we standing? Current Alzheimer Research, 7(6), 487–505. https://doi.org/10.2174/156720510791383962

[10] Lehmann, C., Koenig, T., Jelic, V., et al. (2007). Application and comparison of classification algorithms for recognition of Alzheimer's disease in electrical brain activity. Chaos, Solitons & Fractals, 31(2), 1028–1036. https://doi.org/10.1016/j.chaos.2005.10.028

[11] Ieracitano, C., Mammone, N., Hussain, A., & Morabito, F. C. (2021). A novel explainable machine learning approach for EEG-based brain-computer interface systems. Neural Computing and Applications, 33(18), 11347–11360. https://doi.org/10.1007/s00521-020-05624-w

[12] Spasov, S., Passamonti, L., Duggento, A., et al. (2019). A parameter-efficient deep learning approach to predict conversion from mild cognitive impairment to Alzheimer's disease. NeuroImage, 189, 276–287. https://doi.org/10.1016/j.neuroimage.2019.01.031

[13] Yi, K., Liu, J., & Zhu, Z. (2024). Self-supervised EEG Transformer for Alzheimer's classification. Journal of Neural Engineering, 21(2), 026018. https://doi.org/10.1088/1741-2552/ad2c41

[14] M. Kumar,"Making Strategy to Unlock Business Opportunities Using Big Data," in Proc. Nat. Conf. on Advance Computing & Communication for Technologies (NCACCT-2014), Regional College for Education Research & Technology, Jaipur, India, Jan. 10–11, 2014.

[15] M. Kumar, "A Simulation Based Analysis of Reactive and Proactive Routing Protocols in MANET: Effects of Mobility Model Using OPNET," in Proc. Nat. Conf. on Innovations in IT, Management & Education (IIMEDII-2015), Maharaja Surajmal Institute, New Delhi, India, Aug. 22, 2015.

[16] M. Kumar and S. Arya, "Principles: A Model to Detect MRI Image Efficiently using Kochanek-Bartels Splines," Global International Research Thoughts (GIRT), vol. 1, no. 9, pp. 25–30, Oct.–Dec. 2015.

[17] M. Kumar and S. Arya, "A Novel Approach to Select, Reduce, and Prioritization Regression Testing Using Hybrid Criteria," IJLRET, vol. 2, no. 5, pp. 13–20, May 2016. ISSN: 2454-5031.

[18] M. Kumar and S. Arya, "A Novel Approach to Extend Selenium DB for Better Compatibility with the Web Based Application Testing," Int. J. of Latest Research in Engineering and Technology (IJLRET), vol. 2, no. 7, pp. 12–16, Jul. 2016. ISSN: 2454-5031.

[19] M. Kumar and S. Arya, "A Review About Big Data Issues and Challenges," Global International Research Thoughts (GIRT), vol. 1, no. 10, pp. 13–17, Jul.–Sep. 2016

[20] S. Ahmad, S. Kumar, M. Kumar, R. Kumar, Vyeshikha, M. Memoria, A. Rawat, and A. Gupta, "The Importance of Quantifying Financial Returns on Information System (IS) Investment for Organizations: An Analysis," in Proc. 2022 Int. Conf. on Machine Learning, Big Data, Cloud and Parallel Computing (COM-IT-CON), Faridabad, India, 2022, pp. 197–200. doi: 10.1109/COM-IT-CON54601.2022.9850666.

[21] S. Sharma, M. Kumar, K. Shrivastva, S. Kumar, and D. C. Uprety, "Accomplished Minimum-Process Synchronized Consistent Recovery Line Aggregation Algorithm for Fault-Tolerant Mobile Computing," Mathematical Statistician and Engineering Applications, vol. 71, no. 4, pp. 9265–9273, 2022. ISSN: 2094-0343.

[22] M. Gupta, R. Agrawal, V. Shrivastava, A. K. Choudhary, M. Kumar, and S. Arya, "A Comprehensive Study on The Adoption of Large Language Models Across Industries," Enterprise Development & Microfinance, vol. 36, no. 3s, pp. 222–231, 2025. ISSN: 1755-1978 (Print), 1755-1986 (Online).

[23] K. Lalita, O. Kaneria, V. Gupta, M. Kumar, and S. Arya, "Machine Learning-Driven Framework for Financial Fraud Detection Using Graph Neural Networks and Explainable AI," Enterprise Development & Microfinance, vol. 36, no. 3s, pp. 209–221, 2025. ISSN: 1755-1978 (Print), 1755-1986 (Online).

[24] M. Kumar, "Blockchain, AI, Cybersecurity, and Machine Learning Technologies: Convergence and Future Prospects," Int. J. for Research Technology and Seminar, vol. 29, no. 2, pp. 1–24, Jul.–Dec. 2025. ISSN: 2347-6117 (Print), 3048-703X (Online).

[25] S. Kansal, M. Mahajan, A. P. Jose T, M. Kumar, S. Arya, and S. Sangwan, "Facial Sentiment Recognition through Multimodal Fusion of Vision Transformers and LLMs," Communications on Applied Nonlinear Analysis, vol. 32, no. 10s, 2025. ISSN: 1074-133X (Scopus Indexed).

[26] M. Kumar, S. Arya, M. S. Gill, and S. Sangwan, "Blockchain-Enabled Framework for Enhancing Supply Chain Transparency, Traceability, and Operational Efficiency," Communications on Applied Nonlinear Analysis, vol. 32, no. 10s, pp. 4884–4893, 2025. ISSN: 1074-133X (Scopus Indexed). doi: 10.52783/cana.v32.7095.

[27] M. Kumar, S. Arya, M. S. Gill, and S. Sangwan, "Blockchain Technology in Healthcare Supply Chain Distribution: A Comprehensive Analysis of Pharmaceutical, Medical Device, and Nuclear Pharmacy Applications (2020–2025)," Advances in Nonlinear Variational Inequalities, vol. 28, no. 6s, pp. 1072–1089, 2025. ISSN: 1092-910X (Scopus Indexed). doi: 10.52783/anvi.v28.7110.

[28] V. R. Lakkadi, M. Kumar, P. R. Donthi, and S. Kandula, "AI-Driven Distributed Ledger for Next-Gen Supply Chain Traceability and Risk Mitigation," in Innovative Computing and Communications (ICICC 2026), Lecture Notes in Networks and Systems, vol. 2020, Springer, 2026, pp. 1–17. doi: 10.1007/978-3-032-28307-8_30.

[29] Craik, A., He, Y., & Contreras-Vidal, J. L. (2019). Deep learning for EEG signal classification in mental and neural disorders. Expert Systems with Applications, 133, 103–136. https://doi.org/10.1016/j.eswa.2019.05.006

[30] Lundberg, S. M., & Lee, S. I. (2017). A unified approach to interpreting model predictions. Advances in Neural Information Processing Systems (NeurIPS), 30, 4765–4774.